Proceedings of the IASTED International Conference
Biomedical Engineering (BioMed 2012)
February 15 - 17, 2012 Innsbruck, Austria

KINEMATIC AND KINETIC ANALYSIS OF HUMAN MOTION AS DESIGN INPUT FOR AN UPPER EXTREMITY BRACING SYSTEM

Jakob Karner, Werner Reichenfelser and Margit Gfoehler
Research Group Machine Elements and Rehabilitation Engineering,
Vienna University of Technology, Institute 307/3
Getreidemarkt 9, 1060 Vienna, Austria
jakob.karner@tuwien.ac.at

ABSTRACT
Upper extremity motion in humans is complex and irregular. An orthosis designer cannot count on cyclic procedures or repetitions. When designing a bracing system for the upper limb, this complexity is challenging and therefore it is essential to know about the necessary torques, angular velocities and joint ranges. In this study, we took a closer look at tasks associated with daily living and defined requirements for an upper limb orthotic device. The required working range of the assistive device in order to cover the required range of motion (ROM) was defined. Furthermore, external torques were assessed to facilitate the dimensioning of locking and weight compensation systems and to support strength calculation. The angular velocity at each joint of interest was calculated, as required e.g. for hydraulic component design. Prior to the development of a prototype, an evaluation of the defined joint ranges was envisioned. Additionally we investigated the effect of restricted joint angle ranges on movement performance.

KEY WORDS
Upper limb, orthosis, kinematics, kinetics, torque, range of motion (ROM), angular velocity, human motion analysis, activities of daily living

1. Introduction

The design of an upper extremity bracing system is demanding in many ways. The developer faces multiple challenges such as kinematic misalignment and the design of the interface between human and assistive device [1-2]. Furthermore, joint torques and range of motion (ROM) during movement as well as the angular velocities at the anatomical joints need to be considered.

Upper extremity motion has been studied before and several authors have published data regarding the joint ROM [3-6]. However, little information is available on the angular velocities and torques at each anatomical joint. Murray et al. [7] presented moments and forces impinging on the shoulder and elbow projected on a Cartesian coordinate system. Murphy et al. [8] and Reyes-Guzmán et al. [9] presented peak translational velocities of the end effector (hand) during tasks associated with daily living. Up to date no complete data set on joint ROM, joint torques and joint angular velocities is available for complete daily living tasks.

The European project MUNDUS (Multimodal Neuroprosthesis for Daily Upper Limb Support) aims at developing an assistive framework for recovering direct interaction capability of motor impaired people. Within MUNDUS, actuators modularly combine a lightweight exoskeleton with a weight compensation mechanism, a wearable neuroprosthesis for arm motion and a mechanism to assist grasping. Within this framework, the present work aims at defining the requirements for the exoskeleton. Especially torque characteristics of the human arm, the ROM during four tasks associated with daily living and the angular velocities throughout the complete tasks are pictured. We also show the effect of limited joint ranges on the movement trajectories. Restrictions at the individual degrees of freedom (DoFs) are investigated.

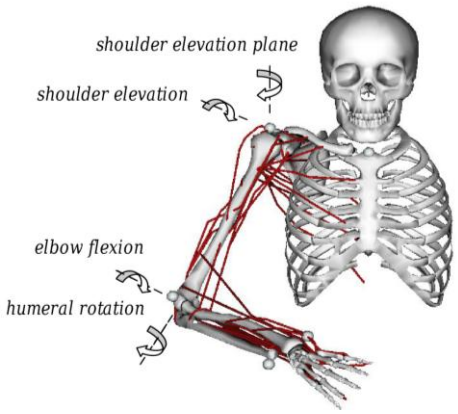

Figure 1. Anatomical model of the shoulder-arm complex. The DoFs of interest, *shoulder elevation plane*, *shoulder elevation*, *humeral rotation* and *elbow flexion*, are pictured. Spheres in white illustrate the virtual markers in the model.

2. Materials and Methods

2.1 Subjects

Fifteen healthy subjects, eleven males and four females with mean age 24.1±1.5 years voluntarily took part in the study. All subjects had a dominant right hand and no upper extremity complaints. Data on the height of the participants was collected by self report. For each subject

DOI: 10.2316/P.2012.764-105

the lengths of forearm and upper arm were measured with elbow 90 degrees flexed and upper arm along the longitudinal axis according to DIN EN ISO 7250-1. Forearm length was defined from the back of the upper arm to the grip centre of the hand. Inclusion criteria were: body dimensions within the 5^{th}-95^{th} percentile and age between 18 and 65 years (DIN 33402-2). Exclusion criteria were: presence of any musculoskeletal or anatomical problem that limits the functionality of the arm.

Median body height was 177.8±8.6cm; upper arm length 363.3±26.1mm and forearm length 354.4±25.4mm. The participants received verbal information on the aim and the procedure of the study and signed written consent forms before participating in the study.

2.2 Instrumentation and Marker Set-up

Motion measurements of activities of daily living (ADL) were recorded using the advanced infrared light based motion capture system Lukotronic (Lutz Mechatronic Technology e.U., Innsbruck, Austria). Two camera units were used with three lenses each and an accuracy of 0.002m. All data was sampled with 100Hz.

According to the model of Rab et al. [10] and the recommendation of the International Society of Biomechanics (ISB) [11], five markers were used to monitor the movement. One marker was placed at the torso (sternum - jugular notch), one at the shoulder (clavicle - acromioclavicular joint), one at the upper arm (humerus - lateral epicondyle) and two at the wrist (radius - styloid process and ulna - head dome). Due to the fact that *shoulder elevation* did not exceed 120°, the acromial method is valid [12-13]. The active markers were attached using double-sided adhesive tape. To avoid artefacts from cable motion and enable undisturbed motion, cables were attached to the body as well. The local coordinate system was defined at the edge of the table and fits to the recommendation of the ISB for the trunk [14]. Thus, the X-axis is directed forward, the Y-axis upward and the Z-axis laterally (right-hand rule).

2.3 Measurement Procedure

Camera position and general measurement set-up were chosen based on previous experience. The distance from chair to table was variable, dependant on the chosen sitting position of the subject (Figure 2) but fixed during the measurement session.
Subjects were seated in a wheelchair. They were instructed to sit comfortable and lean against the backrest, feet on the floor. The initial hand position was defined at the armrest. Prior to the measurements the participants had time to train all planned movements with their dominant right arm.

Each of the four tasks was performed three times by each participant. During the recording, the participants were instructed to sit against the backrest and pause at least for one second at the armrest before starting with the motion. The residual trunk movement was recorded through the sternum marker (Figure 3). Each single task was performed once within nine seconds. The starting and end positions were marked on the table.

The investigated activities of daily living were selected in consultation with clinical staff within the MUNDUS team. Furthermore, two of the ADL, *combing hair* and *drinking*, are often used in motion analysis. The other two tasks, *interacting with own body* and *move other hand*, were considered important by the patients questioned for the study. The chosen tasks do represent other common motions such as eating or personal hygiene.

Combing hair. Start and end position was the initial position at the armrest. The comb is placed at a marked position on the table. Subjects were instructed to perform the motion of combing once, from forehead to the back.

Drinking from bottle with straw. Start and end position at the armrest. Grasping the half litre bottle, full with water and an inserted straw, move to mouth and take one sip. Return bottle to marked position and move to initial position.

Interacting with own body. Same start and end position as described in tasks 1 and 2. The subjects were instructed to scratch at the chest. The target area was defined around the sternum.

Move other hand. Start and end position same as in the other tasks. Left hand is positioned at the left armrest. The right hand grasps the left hand at the wrist and replaces the hand to the left thigh.

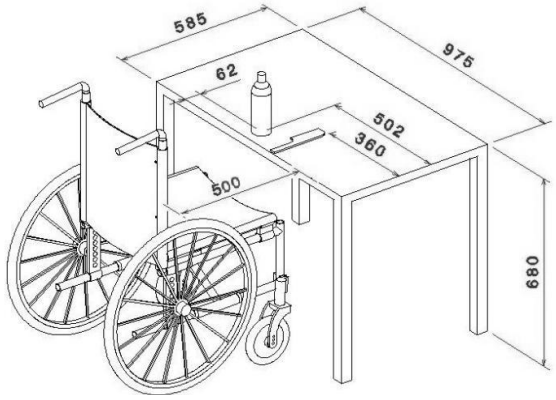

Figure 2. Measurement set-up. Table, tools and wheelchair are assembled as described in the text.

2.4 Data Processing and Analysis

Marker positions in the local coordinate frame were recorded with the Lukotronic software AS202. Custom written software in Matlab (The MathWorks, Inc., Cambridge, MA, USA) was used for modifying the data to feed it into OpenSim [15] for further evaluation. Monotone piecewise cubic interpolation was applied to fill small gaps in the raw data [16]. The kinematic data was filtered with a 2^{nd} order Butterworth filter and a cutoff frequency at 6Hz [17].

An upper extremity model [18] for OpenSim was utilized to perform inverse kinematics (1) and inverse dynamics (2) calculations. Internal properties were added to the used kinematic model and the joint ranges were adapted to the observed ones.

$$\min_{q}\left[\sum_{i\in markers} w_i\|x_i^{exp} - x_i(q)\|^2\right] \quad (1)$$

The optimisation criterion used by OpenSim is shown in (1). The generalised coordinates q are the DoFs, x_i^{exp} denotes the experimental marker positions, the corresponding virtual markers are x_i and the marker weight is w_i. The index *i* indicates the different markers. The weight is a factor to specify how strongly the algorithm minimises the error between measured and virtual marker positions. The inverse kinematic solver tries to match the measured marker positions to the virtually defined markers with minimal error and calculates joint angles over time.

$$\tau = M(q)\ddot{q} - C(q,\dot{q}) - G(q) - F \quad (2)$$

The joint torques were determined using the Newton-Euler equations (2). The vector τ represents the unknown set of joint torques, M(q) is the mass matrix (inertial properties), C(q, $\dot{q}$) is the combination of Coriolis and centrifugal force, G(q) represents the gravity force and F are external forces, in this case the external load at the hand (drinking bottle). The generalised coordinates (DoFs), their velocities and accelerations are represented by q, $\dot{q}$ and $\ddot{q}$.

The joint angular velocities, the joint torques and the ROM during the selected movements were calculated within the simulation software and Matlab scripts. Joint angular velocities and joint torques are calculated for the segments upper arm and forearm accordant the DoFs. At the metacarpal bone a vertical load (5N) was applied to simulate the 500ml water bottle. A simulation of light lifting with 5N was already done in a previous study [7].

Due to hidden markers, some marker recordings showed large gaps. Some recordings had very diverging recording times and thus were not feasible for collective evaluation and standardisation. In total 9.6% of all recordings were dismissed due to large gaps or large time variance. For the analysis of the ROM, valid recordings were standardised over cycle time and averaged over all repetitions and subjects. Measured residual trunk motion was deducted from all tasks. Joint moments were evaluated for the subjects with the largest body dimensions and thus largest moments. Highest and averaged values of angular velocities are pictured.

The optimisation criterion shown in (1) was used to evaluate the effect of restrictions of chosen DoFs for the *drinking* task. The limitations simulate an orthotic device that restrains the performed motion. The inverse kinematic solver determines the best matching set of generalised coordinates with the restricted joint angle ranges and the solution can be compared to the results with unrestricted motion.

3. Results

The joint torques, angles and velocities are presented for *shoulder elevation*, *shoulder elevation plane*, *elbow flexion* and *humeral rotation* (Figure 1). Shoulder positions were chosen as proposed by Doorenbosch et al. [19]. Wrist flexion/extension and radius/ulna deviation were locked at initial position (0°), simulating a rigid wrist orthosis. According to the definitions in the anatomical model, *shoulder elevation* (anteversion), ventral *shoulder elevation plane* (towards shoulder flexion/extension plane), internal *humeral rotation* and *elbow flexion* are positive. Torques due to initial properties and additional forces are negative in the above mentioned orientations.
Figure 3 shows the measured trunk motion of one participant.

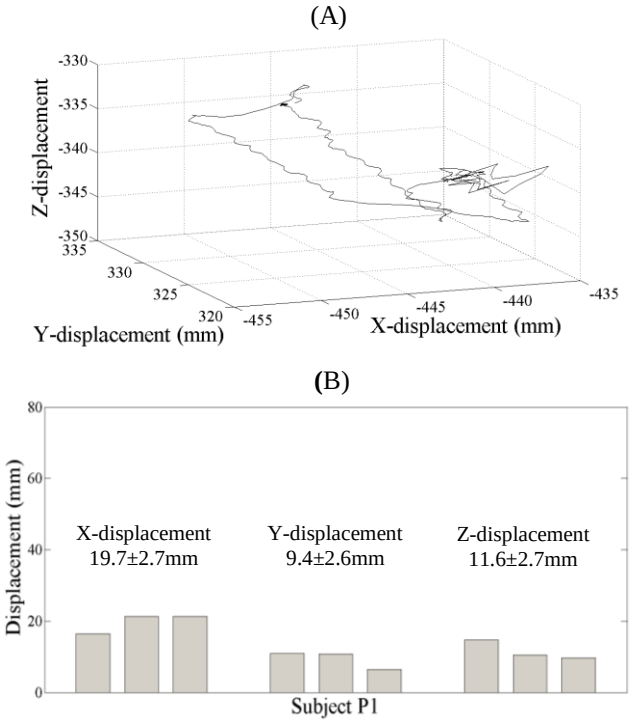

Figure 3. In (A) the residual 3D trunk motion of one subject during the task *drinking* is exemplary pictured. In (B) all three repetitions of the drinking task of this participant are projected on the global coordinate system and grouped. The median ± std is outlined.

3.1 Activities of Daily Living

The graphs pictured in Figures 4-7 show the joint angles ± standard deviation during the selected movements averaged over all subjects and repetitions. All tasks are presented from the starting position to the end position. The observed maximum ROM at the *shoulder elevation plane* was 2.38° to 82.17°, the maximum range at the *shoulder elevation* 19.62° to 55.70°, biggest range of *humeral rotation* was 1.80° to 77.48° and biggest range of *elbow flexion* was 66.97° to 140.80°.

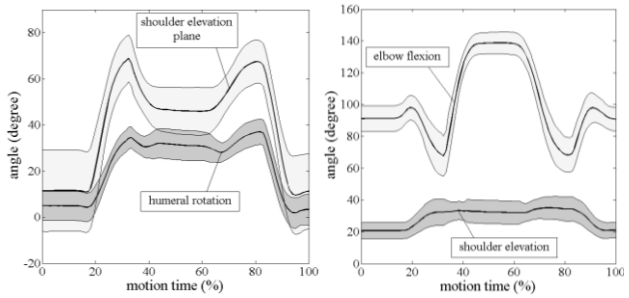

Figure 4. The averaged ROM for the ADL *drinking* is shown. All DoFs are pictured over standardised cycle time.

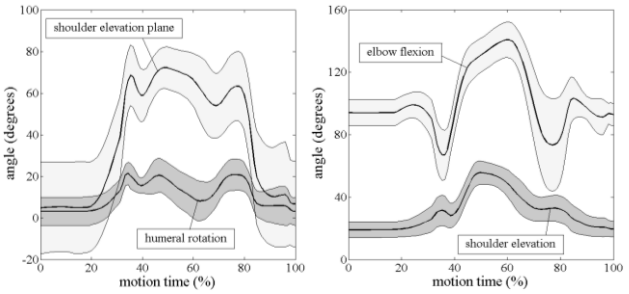

Figure 5.The averaged ROM for the ADL *combing hair* is shown. All DoFs are pictured over standardised cycle time. Especially high *shoulder elevation* was observed.

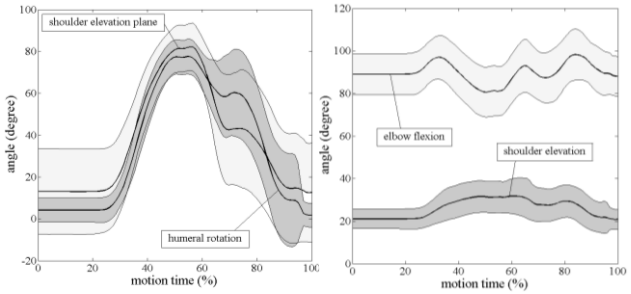

Figure 6.The averaged ROM for the task *move other hand* is shown. All DoFs are pictured over standardised cycle time. High *humeral rotation* was observed during this task.

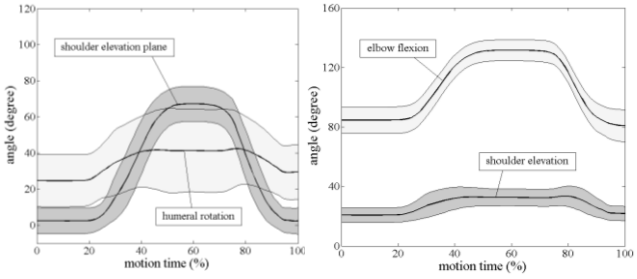

Figure 7.The averaged ROM for the task *interact with own body* is shown. All DoFs are pictured over standardised cycle time. High standard deviation was seen in *humeral rotation*.

The maximum averaged ROM for each of the observed tasks (Figure 4-7) were calculated and summarised in Table 1.

Table 1. Averaged ranges of motion for each task.

DoF\Task	*Drinking*	*Combing hair*
Shoulder elevation	20.75°-35.08°	19.62°-55.70°
Shoulder elevation plane	9.57°-68.83°	4.80°-72.24°
Elbow flexion	67.67°-138.80°	66.97°-140.80°
Humeral rotation	1.80°-37.05°	3.21°-20.81°
DoF\Task	*Move other hand*	*Interact with own body*
Shoulder elevation	20.81°-31.74°	20.80°-33.59°
Shoulder elevation plane	12.53°-82.17°	2.36°-67.34°
Elbow flexion	80.63°-98.26°	80.86°-131.60°
Humeral rotation	1.79°-77.60°	24.81°-42.31°

3.2 Joint Torques

The trajectories in Figures 8-11 show the shoulder and elbow torques of one specific subject while performing all different tasks. In Table 2 the maximum torques at each joint that were found among all subjects and observed motions, are shown. Both, the torques only due to initial properties and torques resulting from an additional external load of 5N were calculated.

Table 2. Maximum torques at each joint are presented. Values calculated with external vertical force (5N) versus no extra load.

DoF	Torque w. Load (Nm)	Torque (Nm)
Shoulder elevation	12.57	7.35
Shoulder elevation plane	3.27	2.64
Elbow flexion	4.15	3.31
Humeral rotation	3.49	2.59

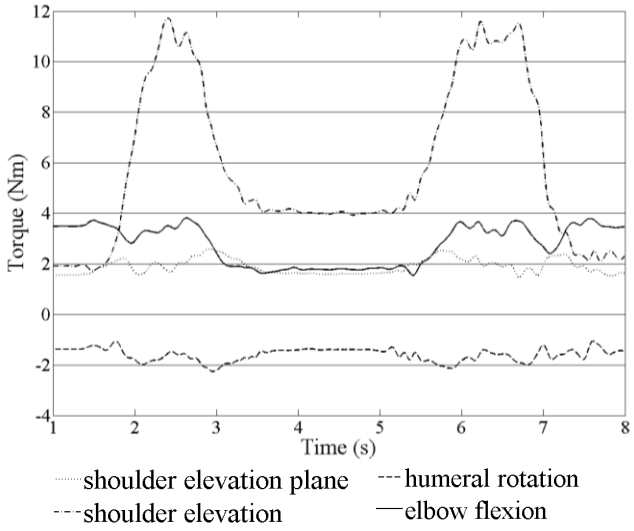

Figure 8. Torque characteristics for all DoFs with additional load during *drinking* are presented.

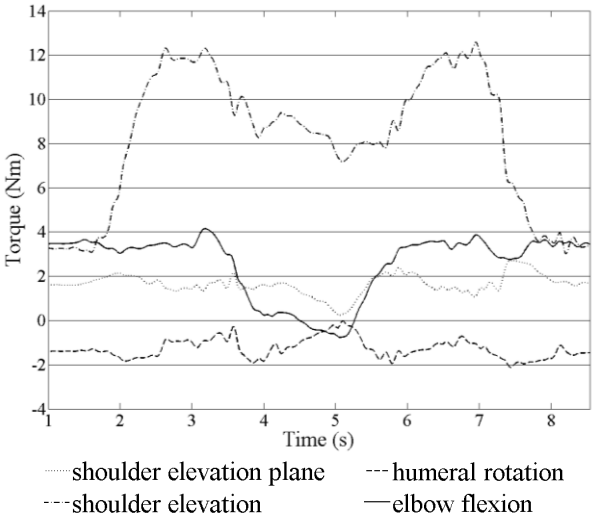

Figure 9. Torque characteristics for all DoFs with additional load during *combing hair* are presented.

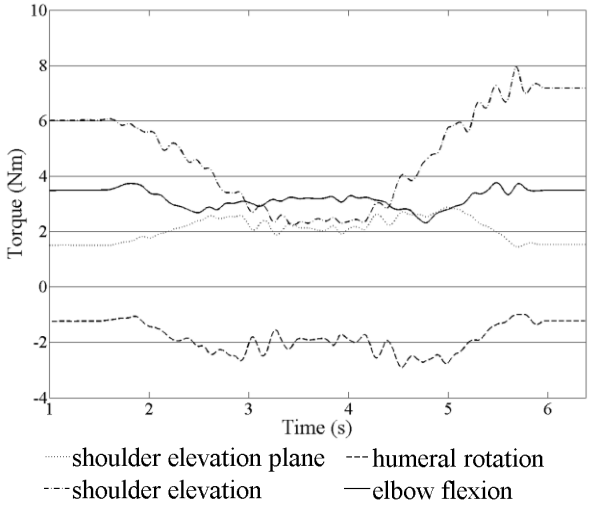

Figure 10. Torque characteristics for all DoFs with additional load during *interact with own body* are presented.

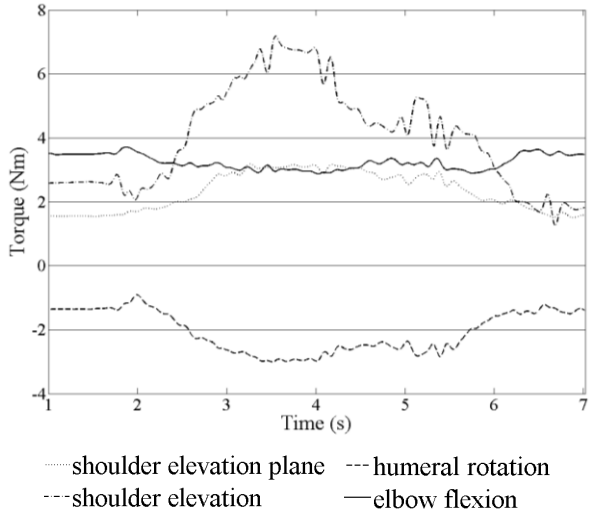

Figure 11. Torque characteristics for all DoFs with additional load during the task *move other hand*s are presented.

3.3 Angular Velocities

In Figures 12-13 angular velocities from the upper arm and forearm during all tasks of the same participant as in Figures 8-11 are presented. The maximum values of the angular velocities and their median ±std. averaged over four participants and all movements are presented in Table 3.

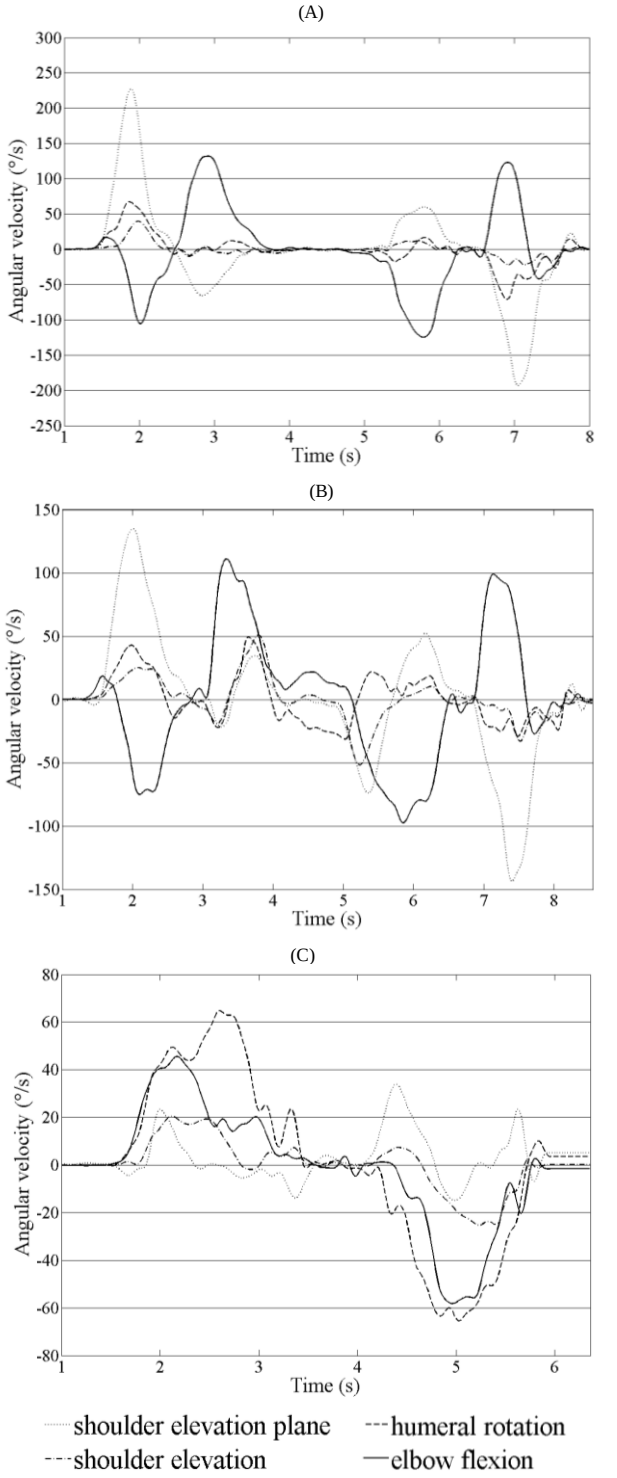

Figure 12. Angular velocities are pictured. The characteristic for one participant is shown for the tasks (A) *drinking*, (B) *combing hair* and (C) *interacting with own body*.

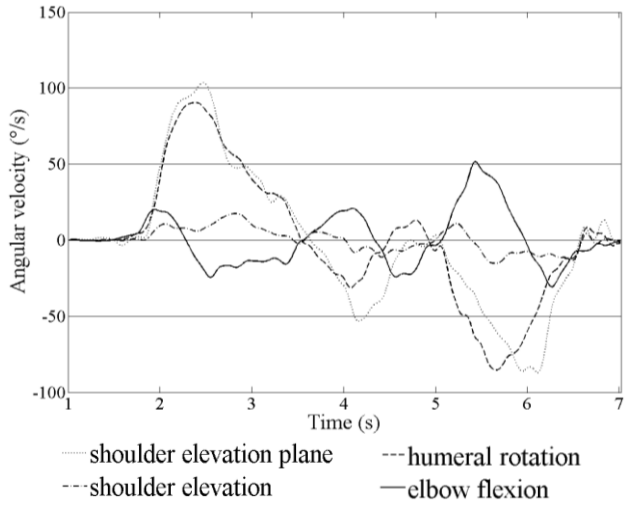

Figure 13. Angular velocities are pictured. The characteristic over *move other hand* for one participant is shown.

Table 3. For each DoF averaged peak velocities ±std. and maximum peak velocities of four randomly chosen subjects are given.

DoF	Ang. vel. (°/s)	Max. ang. vel. (°/s)
Shoulder elevation	100.62±51.2	227.80
Shoulder elevation plane	33.97±18.6	81.67
Elbow flexion	97.73±37.5	181.01
Humeral rotation	83.21±24.8	133.64

3.4 Comparison – Restricted and Unrestricted DoF

The exemplary task *drinking* which is shown above is used to analyse the effect of restrictions to selected DoFs. From the measured ROM we were able to suggest joint ranges for a bracing system. We analysed the consequence of using an orthosis with restricted joint angle ranges. The resulting movement trajectories were compared to the measured ROM.

First, the *elbow flexion* was set to 0°-120°. Additionally, the *humeral rotation* was locked at positions from 20° to 70° in increments of 10°. Then the simulation was repeated with *elbow flexion* restricted to 0°-140°. In both cases the *shoulder elevation* was set to 25°-75° and the *shoulder elevation plane* to 0°-110°. Wrist flexion/extension and radius/ulna deviation were always locked at initial position (0°).

The resulting joint trajectories from simulations with restricted joint ranges were compared to those with unrestricted joints. In each calculation the optimisation algorithm tried to find a set of generalised coordinates (joint angles) that minimises the error between the virtual markers in the model and the measured marker positions in the experiments. Figure 14 exemplary shows the 3D trajectory of the metacarpal bone during the movement *drinking*; the target position is the mouth. The whole task from initial position to bottle, to mouth, back to the table and back to the starting position is pictured. Without any restrictions of the joint ranges the minimum distance between mouth and metacarpal bone during *drinking* was 126.69mm. With restricted joint angle ranges the minimum distance was 146.83mm, that means an increase of 15.9%. In Figure 15 projections on the body planes are visualised. The trajectory of the metacarpal bone is presented in the sagittal, coronal and transversal planes.

Dependant on the chosen setting (DoFs) a detailed list of the resulting minimum distances to the target point is given in Table 4. Changes in *elbow flexion* effect the resulting distance between metacarpal bone and target position (mouth) more than changes in *humeral rotation*.

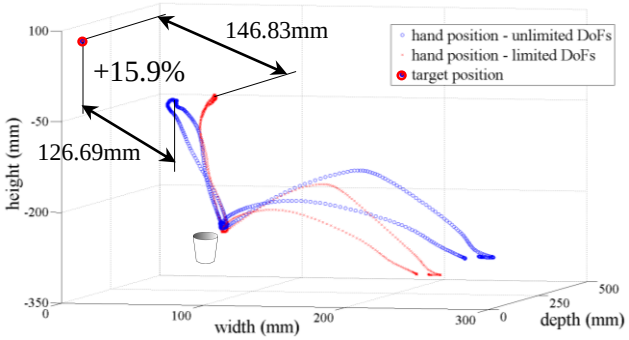

Figure 14. Comparison between limited and unlimited DoFs. Both trajectories reflect the whole motion *drinking*. The distance between endpoint of the movement and target position is shown. The absolute discrepancy extends about 15.9% or 20.14mm.

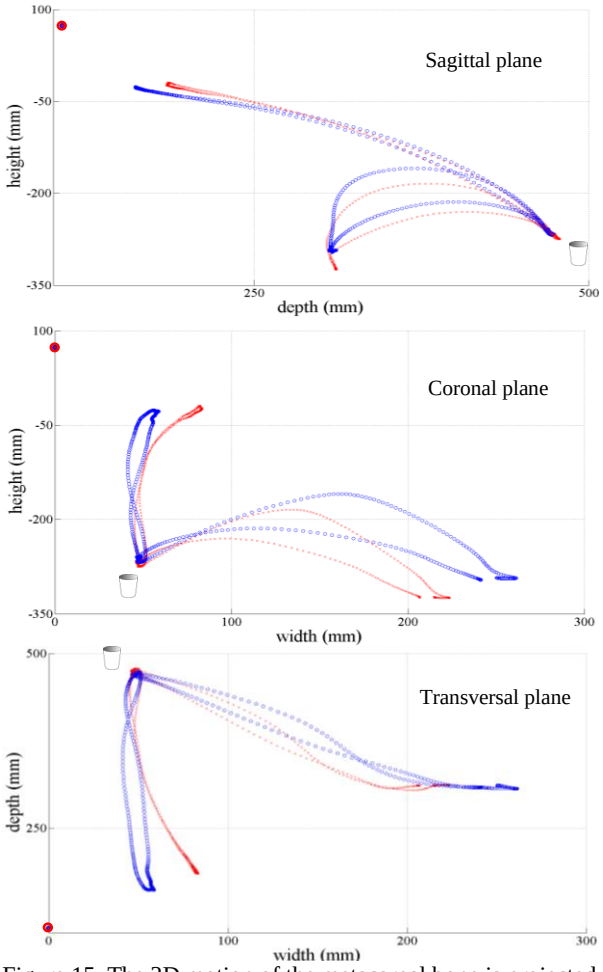

Figure 15. The 3D motion of the metacarpal bone is projected on the body planes. The sagittal plane is seen laterally, the coronal plane from dorsal and the transversal plane from coronal.

Table 4. The calculated minimal displacements between metacarpal bone and mouth depending on the range of motion at the DoFs are listed. The increase of the displacement in relation to the unlimited motion is given in mm. Ratios in % are listed in relation to the minimum distance of unlimited motion.

Fixed *humeral rotation*	*Elbow flexion* range	Minimal displacement *limited* (mm)	Increase of displacement (mm)	Ratio *unlimited* to *limited* (%)
70°	0°-120°	238.94	112.25	188.60
60°	0°-120°	216.57	89.88	170.94
50°	0°-120°	213.97	87.28	168.89
40°	0°-120°	217.15	90.46	171.40
30°	0°-120°	232.73	106.04	183.70
20°	0°-120°	248.92	122.23	196.48
70°	0°-140°	162.70	36.01	128.42
60°	0°-140°	147.55	20.86	116.47
50°	0°-140°	135.86	9.17	107.24
40°	0°-140°	133.28	6.59	105.20
30°	0°-140°	146.83	20.14	115.90
20°	0°-140°	162.00	35.31	127.87

4. Conclusion and Discussion

Investigating daily living activities helps to understand human motion and to get an insight into the demanding task of developing a bracing system for the upper extremity. With our focus on orthotic design we combined motion capture technologies and simulations to assess requirements for an assistive device. The recorded motion data and an anatomical upper limb model were used for further analysis of joint torques and angular velocities. Essential joint ranges and maximum torques were defined. The angular velocities during the analysed motions were calculated and reported.

The participants were seated in a wheelchair with initial hand position at the arm rest. This of course influences the joint angles in starting position and the ROM especially at *elbow flexion* and at *shoulder elevation*.

The inevitable study set-up and the analysis of complete motions, including tasks like *taking brush* or *bottle*, make a reasonable comparison with recent publications difficult. Van Andel et al. [5] and Magermans et al. [4] recorded data only from initial position to target position and excluded sections like *taking brush*. The maximum angles we observed at the elbow joint and *humeral rotation* were consistent with data from van Andel et al. but the presented data shows rather higher values for shoulder flexion. Compared to the results from Magermans et al. [4] we found that our values for the *shoulder elevation* during *drinking* are lower. This may be due to the drinking bottle used instead of a spoon.

The *drinking* task and the *combing hair* motion showed large ranges of motion at the elbow joint. On average 140° were necessary to achieve the tasks. In contrast to *drinking* higher values of *shoulder elevation* (on average 55.7°) were observed during *combing hair*. Tasks where the hand is moved to the mouth need less *shoulder elevation* to be completed than tasks where the hand is moved above the mouth. Similar to Magermans et al. [4] the importance of *elbow flexion* for feeding tasks was observed. *Interacting with own body* provides high *elbow flexion* (on average 131.6°) as well. Around 90° *elbow flexion* was observed for *interact with own body*. Only for the task *move other hand* high values of *humeral rotation* (on average 77.6°) were seen. In all other motions *humeral rotation* was roughly between 0° and 40° (Table 1). Due to inaccurate specification of the target point at the sternum the motion *interacting with own body* showed large standard deviation especially for *humeral rotation*. In each of the investigated tasks wide ranges (2.36°-82.17°) for *shoulder elevation plane* were noted. During all recordings the trunk motion was very small (Figure 3).

The torques published by Murray et al. [7] were in the same ranges as the moments we calculated here. Unfortunately they introduced Cartesian coordinate systems at the shoulder and elbow joints and projected their results. More easily applicable for design are torque values at each DoF.

To estimate the maximum joint torques that may occur, measured data of the subjects with largest upper arm length and largest forearm length were evaluated. An additional load of 5N, simulating the weight of a 500ml water bottle, was applied at the metacarpal bone.

Obviously the highest moments were found at the shoulder joint (Table 2) during the tasks *combing hair* and *drinking* where the hand was moved distally to grip the comb/bottle. During *interact with own body* the lowest maximum shoulder torque (~7.5Nm, Figure 10) was generated. Torques at the *shoulder elevation plane*, *humeral rotation* and *elbow flexion* were very constant among the different tasks. Only the *combing hair* task showed large changes in the elbow torque. The additional load of 5N results in a rise of the torque of 41.5% at the shoulder. Less influence was seen at the elbow, *shoulder elevation plane* and *humeral rotation* (19.2% to 25.79%).

Looking at the distribution of the angular velocities during the different tasks, two patterns were seen. On the one hand for motions moving the hand to the mouth or higher, angular velocities at the *shoulder elevation* and *elbow flexion* seem very dominant and on the other hand, for lower hand positions the velocity of *humeral rotation* is very controlling. In general the averaged angular velocities are much lower than the observed maximum values (Table 3) and especially during the grasping phase low velocities were observed. Generally, angular velocities are low in the regions where high torques are generated (*move other hand* around 3.5sec or *drinking* at 2.5sec.). Buckley et al. [3] reported that joint velocities are much higher than those usually used in prosthetics research.

To assess the influence of the orthotic device on specific movements we performed simulations with limited joint ranges and locked DoFs. We investigated the

influence of limited elbow joint range (maximum flexion 120°/140°) and of fixing *humeral rotation* at angles between 20° and 70°.

We observed that the influence of limited *elbow flexion* is much higher than locked *humeral rotation*. Limited *elbow flexion* can e.g. occur when using restraining straps at the biceps brachii or hindering mechanical components like cuffs. The minimum distance between target point and metacarpal bone (end effector) during the unlimited motion was 126.69mm. This distance was taken as optimum. Figures 14-15 show the resulting difference with locked DoF *humeral rotation* (30°) and elbow joint range 0°-140°. Because of the diverging joint ranges already the calculated starting position (results from the inverse kinematics) of the effector is different (Figure 14-15). The optimisation criterion led to a matching position at the median target point (drink bottle) at the end point the distance was +15.9% increased in comparison to the unrestricted motion.

In Table 4 increased displacements in comparison to the unlimited motion and the ratios between unrestricted and restricted motion over all calculations are listed.

Limited joint angle ranges at one joint may lead to compensatory movements at other joints. For a limitation of the elbow joint extensive *shoulder elevation* was seen. The locked *humeral rotation* results in an increased motion in the *shoulder elevation plane*. The evaluation showed that it is most essential to cover the start and end positions, as already proposed in [3]. An end effector based solution seems more realistic for a lightweight and inconspicuous design for braces.

The best fitting solution for our bracing system was a setting with *humeral rotation* locked at 40° and 0°-140° *elbow flexion* range. At least 0°-110° for *shoulder elevation plane* and *shoulder elevation* from 25° to 75° are necessary. Simulations with these joint angle ranges showed similar behaviour as simulations with the unlimited setting, only 5.2% additional displacement was observed for the *drinking* task.

Acknowledgements

This work is part of the European Project MUNDUS and was funded by the call EC FP7 ICT 2009-4. The authors also gratefully acknowledge Clara Bock and Michael Hilgert for their help with the measurements and would like to thank all the volunteers that participated in this study.

References

[1] M.A. Buckley, Computer simulation of the dynamics of a human arm and orthosis linkage mechanism. *Proc Instn Mech Engrs*, 1997,349-357.

[2] A. Schiele, An Explicit Model to Predict and Interpret Constraint Force Creation in pHRI with Exoskeletons. *IEEE International Conference on Robotics and Automation*, Pasadena, 2008,1324-1330.

[3] M.A. Buckley, Dynamics of the Upper Limb During Performance of the Tasks of Everyday Living - a Review of the Current Knowledge Base, *Journal of Engineering in Medicine , 210* (Part H), 1996, 241-247.

[4] D.J. Magermans, E.K. Chadwick, H.E. Veeger, & F.C. van der Helm, Requirements for upper extremity motions during activities of daily living, *Clinical Biomechanics,20*, 2005, 591-599.

[5] C.J. van Andel, N. Wolterbeek, C.A. Doorenbosch, D.H. Veeger, & J. Harlaar, Complete 3D kinematics of upper extremity functional tasks, *Gait & Posture,27*, 2008, 120-127.

[6] K. Petuskey, A. Bagley, E. Abdala, M.A. James, & G. Georg, Upper extremity kinematics during functional activities:Three-dimensional studies in a normal pediatric population, *Gait & Posture, 25*, 2007, 573-579.

[7] I.A. Murray and G.R. Johnson, A study of the external forces and moments at the shoulder and elbow while performing every day tasks, *Clinical Biomechanics, 19*, 2004, 586–594.

[8] M.A. Murphy, K.S. Sunnerhagen, B. Johnels, & C. Willén,Three-dimensional kinematic motion analysis of a daily activity drinking from a glass: a pilot study, *Journal of NeuroEngineering and Rehabilitation*, 3:18, 2006.

[9] A. de los Reyes-Guzmán, A. Gil-Agudo, B. Peñasco-Martín, M. Solís-Mozos, A. del Ama-Espinosa, & E. Pérez-Rizo, Kinematic analysis of the daily activity of drinking from a glass in a population with cervical spinal cord injury, *Jounrnal of Neuroengineering and Rehabilitation*, 7:41, 2010.

[10] G. Rab, K. Petruskey, & A. Bagley, A method for determination of upper extremity kinematics, *Gait and Posture, 15*, 2002, 113-119.

[11] S. Van Sint Jan, *Color Atlas of Skeletal Landmark Definitions - Guidelines for Reproducible Manual and Virtual Palpations* (Edinburgh: Churchill Livingstone Elsevier, 2007).

[12] A.R. Karduna, P.W. McClure, L.A. Michener, & B. Sennett, Dynamic Measurements of Three-Dimensional Scapular Kinematics: A Validation Study, *Journal of Biomechanical Engineering, 123*, 2001, 184-190.

[13] C.G. Meskers, M.A. van de Sande, & J.H. de Groot, Comparison between tripod and skin-fixed recording of scapular motion. *Journal of Biomechanics, 40*, 2007, 941-946.

[14] G. Wu,F.C. van der Helm, D.H. Veeger, M. Makhsous, P. van Roy, C. Anglin, et al., ISB recommendation on definitions of joint coordinate systems of various joints for the reporting of human joint motion—Part II: shoulder, elbow, wrist and hand, *Journal of Biomechanics, 38*, 2005, 981–992.

[15] S.L. Delp, F.C. Anderson, A.S. Arnold, P. Loan, A. Habib, C.T. John, et al., OpenSim: Open-Source Software to Create and Analyze Dynamic Simulations of Movement, *IEEE Transactions on Biomechanical Engineering*, *54*(11), 2007, 1940-1950.

[16] F.N. Fritsch, & R.E. Carlson, Monotone Piecewise Cubic Interpolation, *SIAM Journal on Numerical Analysis*, *17*(2), 1980, 238-246.

[17] D.A. Winter, *Biomechanics and Motor Control of Human Movement* (Hoboken New Jersey: John Wiley and Sons, 2005).

[18] K.R. Holzbaur, A Model of the Upper Extremity for Simulating Musculoskeletal Surgery and Analyzing Neuromuscular Control, *Annals of Biomedical Engineering*, *33*(6), 2005, 829–840.

[19] C.A.M. Doorenbosch, J. Harlaar, D.H.E.J. Veeger, The globe system: An unambiguous description of shoulder positions in daily life movements, *Journal of Rehabilitation Research and Development, 40*(2), 2003, 147-156.